Pressure-induced irreversible phase transition in $KSc(MoO_4)_2$

G. D. Saraiva,[1] M. Maczka,[2] P. T. C. Freire,[1] J. Mendes Filho,[1] F. E. A. Melo,[1] J. Hanuza,[2,3] Y. Morioka,[4]
and A. G. Souza Filho[1,*]

[1]*Departamento de Física, Universidade Federal do Ceará, P.O. Box 6030, Fortaleza-CE, 60455-900, Brazil*
[2]*Institute For Low Temperature and Structure Research, Polish Academy of Science, P.O. Box 1410, 50950 Wroclaw, Poland*
[3]*Faculty of Industry and Economics, University of Economics, 118/120 Komandorska Str., 53-345 Wroclaw, Poland*
[4]*Department of Chemistry, Faculty of Science, Saitama University, Shimo-Okubo 255, Urawa, 338-8570, Japan*
(Received 28 February 2003; published 24 June 2003)

We have studied the layered double molybdate $KSc(MoO_4)_2$ under high pressure through Raman scattering experiments. At about 2.0 GPa we observed drastic changes in the Raman spectra associated with a structural phase transition. The high-pressure phase is characterized by the presence of a large number of Raman modes, thus indicating that the high-pressure phase has a lower symmetry than the starting trigonal phase. By performing lattice-dynamics calculations for the trigonal phase we have been able to make a definite assignment of the various Raman modes observed in the experiments, and to get fundamental insights about the mechanism driving the structural modifications in molybdates that are associated with the electrostatic repulsion between the oxygen atoms due to the decreasing of Mo–O bonds and O–O distances. Upon releasing pressure the spectrum of the starting trigonal phase was not recovered, thereby indicating that pressure induced an irreversible phase transition in the $KSc(MoO_4)_2$ crystal.

I. INTRODUCTION

Molybdate materials comprise a large class of inorganic compounds, that exhibit interesting physical properties thus having technological applications in the field of catalysis and quantum electronics.[1] Some members of this class of materials exhibit pressure induced amorphization phenomenon thus making molybdate compounds good prototypes to get new concepts about the physics of amorphization processes and about chemical decomposition under high pressure as well.[2,3]

The double molybdates with chemical formula $M^+M^{3+}(MoO_4)_2$, where $M^+=$Na, K, Rb, Cs and $M^{3+}=$Al, In, Sc, Cr, have been studied owing the richness of structural instabilities induced either by temperature or hydrostatic pressure found in these materials.[4–7] Previous temperature dependent studies of a number of isostructural trigonal molybdates and tungstates revealed an unusually narrow stretching mode of the $(Mo/W)O_4^{2-}$ units always observed in a very narrow frequency range (926–931 cm^{-1}). The $(Mo/W)O_4^{2-}$ units in the trigonal phase have two nonequivalent oxygen atoms, namely, O1 and O2 for the oxygen atoms relying closest to M^+ and M^{3+} cations, respectively (see Fig. 1). Striking is the fact that both frequency and linewidth for this narrow mode are almost temperature independent being not affected by the ferroelastic phase transitions found in these compounds.[6,8] Since the interaction between the tetrahedra units are the main responsible for the different structural phases found in the molybdates, it is fundamental to investigate the relationship between this narrow mode and the tetrahedra configuration in order to gain fundamental insights on the driving mechanism of the structural changes observed in these materials. A way for probing the tetrahedra interaction is by applying hydrostatic pressure and since the Raman spectra are very sensitive to chemical bond changes,

a high-pressure Raman study is very promising for probing the tetrahedra interaction and the nature of this *narrow* mode.

In this work we study the layered double molybdate $KSc(MoO_4)_2$ single crystals under high-pressure through Raman spectroscopy. This compound is well-known for its complex temperature-induced phase transition sequence.[5,9,10] The $KSc(MoO_4)_2$ Raman spectrum presents such a very narrow stretching mode with linewidth of 2.5 cm^{-1} at room temperature. Our study showed that the narrow stretching mode, observed at 926 cm^{-1} for $KSc(MoO_4)_2$, exhibits no pressure dependence for both frequency and linewidth. Lattice dynamics calculations performed within the partial ionic model have allowed us to come up with a definite assignment of the various vibration modes. The narrow mode was assigned to an antisymmetric stretching of the Mo–O1 bond whose length does not change with compression, while the modes associated with the Mo–O2 bond are highly affected
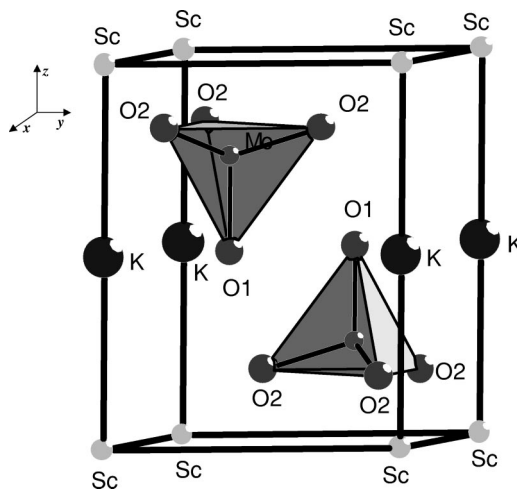

FIG. 1. Unit cell of $KSc(MoO_4)_2$ in the trigonal phase (space group D_{3d}^3). The threefold axis passes through the M–O1 bond.

TABLE I. Factor group analysis for the D_{3d} symmetry.

D_{3d}	$n(N)$	$n(T)$	$n(T')$	$n(L)$	$n(i)$	Activity IR	Activity Raman
A_{1g}	4	0	1	0	3		$xx+yy,zz$
A_{2g}	1	0	0	1	0		
E_g	5	0	1	1	3		$xz,xx-yy,xy,yz$
A_{1u}	1	0	0	1	0		
A_{2u}	6	1	2	0	3	z	
E_u	7	1	2	1	3	x,y	

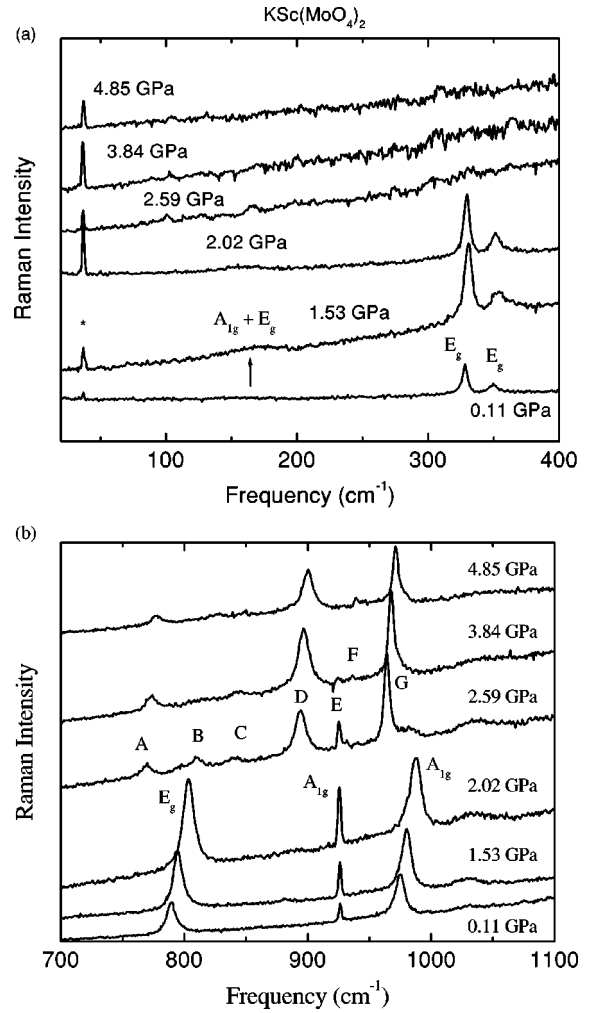FIG. 2. Raman spectra of $KSc(MoO_4)_2$ crystals recorded at different pressures during compression experiments. The upper(lower) panel shows the low(high) frequency regions of the spectra. The peak marked with an asterisk in (a) stands for a plasma line from the laser source.

by compression. At about 2.0 GPa pressure a drastic change in the Raman spectra (increase in the number of Raman modes) indicated a phase transition to a lower symmetry phase. The structural instability has its origin in the electrostatic repulsion between the oxygen atoms due to the decreasing of Mo–O2 bonds and O–O distances. By releasing the pressure, this low symmetry phase remains stable thus indicating that the pressure induced an irreversible phase transition in $KSc(MoO_4)_2$. By combining high-pressure Raman studies with lattice dynamics calculations we have achieved a step forward in the understanding the structural changes of the molybdates and tungstates and their driving mechanisms.

II. EXPERIMENT

Single crystals of $KSc(MoO_4)_2$ were grown by cooling of the molten mixture containing $KSc(MoO_4)_2$ and solvent $K_2Mo_2O_7$ in 1:1 ratio. The cooling rate was 2 K per hour. The pressure dependent Raman spectra were obtained with a triple-grating spectrometer (Jobin Ivon T64000) equipped with a N_2-cooled charge coupled device (CCD) detection system. The line 488.0 nm of an argon ion laser was used as excitation. An Olympus microscope lens with a focal distance $f=20.5$ mm and numeric aperture N.A.$=0.35$ was used to focus the laser beam on the sample surface. High-pressure Raman experiments were performed using a diamond anvil cell (DAC) with 4:1 methanol : ethanol mixture as the transmitting fluid. The pressure calibration was achieved by using the well known pressure shift of the ruby luminescence lines. The spectrometer slits were set for a resolution of 2 cm^{-1}.

III. RESULTS AND DISCUSSION

In order to analyze the results, we first describe the symmetry and vibrational properties of $KSc(MoO_4)_2$ crystals at room temperature. This material crystallizes in a trigonal structure with space group D_{3d}^3 ($P\bar{3}m1$) with one formula per unit cell ($Z=1$).[11] The unit cell is shown in Fig. 1. The Raman active modes at the Γ-point (see Table I) are distributed among the irreducible representations of the factor group D_{3d} as

$$\Gamma_{\text{Raman}}=4A_{1g}+5E_g. \tag{1}$$

The Raman spectra of $KSc(MoO_4)_2$ crystals measured at several pressures are shown in Fig. 2. The low frequency region is shown in Fig. 2(a) and the high frequency region in Fig. 2(b). From the six predicted Raman active internal modes [$n(i)$ in Table I], we have observed five of them. The mode symmetry assignment can be easily achieved by comparison with other molybdates and tungstates compounds.[6,8,12] The modes observed at $975(A_{1g})$, $926(A_{1g})$, $788(E_g)$ are stretching modes whereas bands observed at $327(E_g)$ and $348(E_g)$ cm^{-1} are bending modes. The missing bending mode of A_{1g} symmetry, absent in our spectra due to its very low intensity, is expected to be observed at about 360 cm^{-1} as it does in $KSc(WO_4)_2$ tungstate.[12] The observed band at about 160 cm^{-1} [up arrow in Fig. 2(a)] is related to two overlapped MoO_4^{2-} translational modes with $A_{1g}\oplus E_g$ symmetry. A librational mode is expected to be observed at about 60 cm$^{-1}(E_g)$ but the weak Raman signal from the tiny sample piece inside the pressure cell did not allow us to observe this mode.[5]

In order to assign the Raman peaks to the atomic vibra-

TABLE II. Potential parameters used for the lattice dynamics calculations of $KSc(MoO_4)_2$.

Ion	z (e)	a (Å)	b (Å)	c (kcal$^{1/2}$ Å^3 mol$^{-1/2}$)
K	0.6	1.705	0.09	15
Sc	2.2	1.034	0.08	0
Mo	2.8	0.814	0.09	0
O	−1.05	1.926	0.16	20

Ionic pair	D_{ij} (kcal mol^{-1})	β_{ij} (Å)	r_{ij}^* (Å)
Mo–O	28.0	2.3	2.0

tions accordingly, we performed lattice dynamics calculations to predict both frequencies (eigenvalues) and atomic displacements (eigenvectors) for each Raman active normal mode. Since the $KSc(MoO_4)_2$ is mostly ionic, we performed the calculations on the basis of a partially ionic model described in Ref. 13. The atomic positions used in the calculations were taken from x-ray data.[11] The following interatomic potential was used in the lattice dynamics calculations:

$$U_{ij}(r_{ij}) = \frac{z_i z_j e^2}{r_{ij}} + (b_i + b_j)\exp\left[\frac{(a_i + a_j - r_{ij})}{(b_i + b_j)}\right] - \frac{c_i c_j}{r_{ij}^6}$$
$$+ D_{ij}(\exp[-2\beta_{ij}(r_{ij} - r_{ij}^*)]$$
$$- 2\exp[-\beta_{ij}(r_{ij} - r_{ij}^*)]). \quad (2)$$

This interatomic potential consists of a Coulomb interaction (first term) to model the long-range interactions; a Born–Mayer-type repulsive interaction (second term) for accounting the short-range forces; a van der Waals attractive interaction (third term) to model the dipole–dipole interaction; and finally the Morse potential contribution (last term) to take into account the covalent bond character. z_i and z_j are the effective charges of the ions i and j, respectively, separated by the distance r_{ij}. The parameters (a_i, a_j) and (b_i, b_j) correspond to the ionic radii and ionic stiffness, respectively. The parameters used in the present calculations are listed in Table II. Since we consider covalency for the Mo–O bond only, D_{ij}, β_{ij}, and r_{ij}^* are given for this bond only. The values of the parameters for O atoms as well as the parameter c for K atoms are taken from Ref. 13. The remaining parameters were set to such values shown in Table II in order to obtain the best agreement between the observed [Raman and infrared (not discussed here) results] and calculated frequencies. It is worth noting that it was necessary to adopt lower effective charges of the O atoms (-1.0) than reported for the titanium layered perovskites (-1.2) (Ref. 13) in order to obtain reasonable agreement with the experimental data. This indicates that the Mo–O bonds in $KSc(MoO_4)_2$ are more covalent than the Ti–O bonds in layered perovskites.[13]

The vibrational frequencies of all the observed and calculated Raman active modes along with their symmetries and

TABLE III. Observed and calculated Raman frequencies of the MoO_4^{2-} tetrahedra for the $KSc(MoO_4)_2$ trigonal structure along with their symmetry and assignments [symmetric stretching (ν_1), asymmetric stretching (ν_3), symmetric bending (ν_2), asymmetric bending (ν_4), translation (T') and libration (L)].

Symmetry	Frequency (cm^{-1}) Observed	Calculated	Assignment MoO_4 unit
A_{1g}	975	958	ν_1
A_{1g}	926	918	ν_3
E_g	788	795	ν_3
A_{1g}	. . .	560	ν_4
E_g	348	458	ν_2
E_g	327	331	ν_4
A_{1g}	∼160	171	T'
E_g	∼160	190	T'
A_{1g}	. . .	134	L

assignments are listed in Table III. The atomic displacement vectors for each Raman active normal mode of $KSc(MoO_4)_2$ are shown in Fig. 3. The results of the lattice dynamics calculations confirm the previous assignment of vibrational modes based on other molybdates and tungstates compounds. It is worth noting that the calculations show a very significant difference among the 926 cm^{-1} and the 975 and 788 cm^{-1} stretching modes. As one can see in Fig. 3, the 926 cm^{-1} mode involves a very large stretching motion of the Mo–O1 bond which projects into the interlayer whereas the two remaining stretching modes (975 and 788 cm^{-1}) involve large stretching motions of the Mo–O2 bonds. This feature explains the observed strong intensity polarization dependence of these modes, i.e., the 926 cm^{-1} mode was observed for all studied trigonal molybdates and tungstates as a strong mode for the zz and weak for the xx polarization whereas an opposite behavior was noticed for the remaining stretching modes.[5,6,8] The results of the calculations show also that a very small linewidth of the 926 cm^{-1} mode can be explained by the fact that the Mo–O1 bonds interacts only with the K^+ cations. Since these interactions are very weak, as evidenced through the long K–O1 distance (3.34 Å) which is larger than the sum of ionic radii for O^{2-} and K^+ (1.40+1.64=3.04 Å), the 926 cm^{-1} mode involving stretching motions of mainly Mo–O1 bonds is characterized by very weak anharmonicity. This is further supported by the temperature dependence of both frequency and linewidth observed in others double molybdates and tungstates.[6,8] Now that we get a clear picture of the vibrational properties of $KSc(MoO_4)_2$ through the lattice dynamics analysis we are in a position to discuss the effects of hydrostatic pressure on the structural and vibrational properties of this compound.

On applying pressure, the Raman spectra remains qualitatively the same up to 2.02 GPa, unless for the upshift experienced for all modes due to compression. For pressures larger than 2.02 GPa new and remarkable features become evident in the Raman spectra. The peaks at 327 and 348 cm^{-1} disappears and several weak peaks [not clear in the scale show in Fig. 2(a)] show up in the spectra. We will return to discuss these weak peaks later on. Also, peaks la-
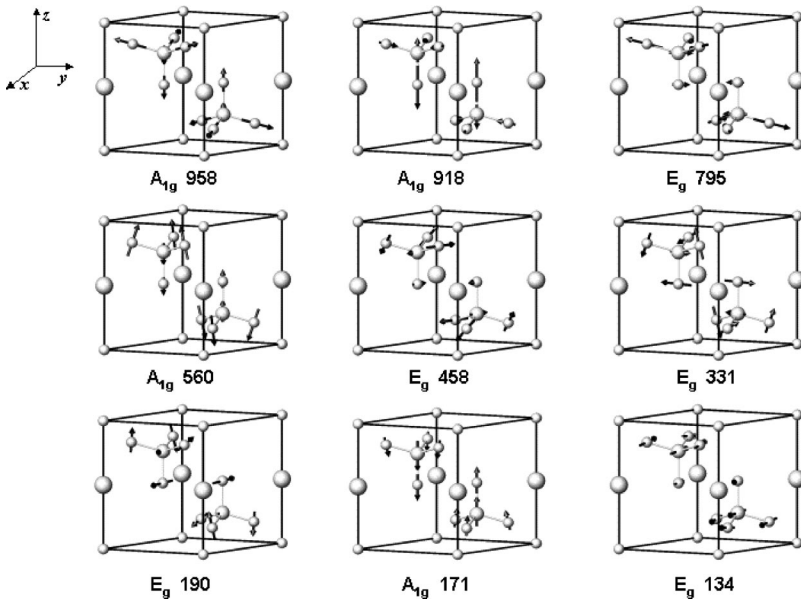
FIG. 3. Eigenvectors for the calculated Raman active modes in the $KSc(MoO_4)_2$ crystal. Sc and K atoms do not move for the Raman active modes in the trigonal phase.

beled A, B, C, D, E, F, and G (see Figs. 2 and 4) show up in the spectra at $P=2.59$ GPa and the peak at 975 cm^{-1} (A_{1g}), from the trigonal phase, disappears. The narrow peak at 926 cm^{-1} decreases in intensity gradually with pressure and it is very weak for $P>3.84$ GPa. No other changes were observed upon compression up to the maximum pressure value of 4.85 GPa reached in our experiments. The main changes observed in the spectra can be followed by analyzing the frequency (ω) vs pressure (P) plot shown in Fig. 4. The results shown in Fig. 4 clearly indicate that the material experiences a structural modification at about $P=2.21$ GPa. All the peaks presents a linear behavior $\omega(P)=\omega_0+\alpha P$ and both frequency intercepts and pressure coefficients are shown in Table IV for the most intense modes. It is noticeable that the modes from trigonal phase exhibit
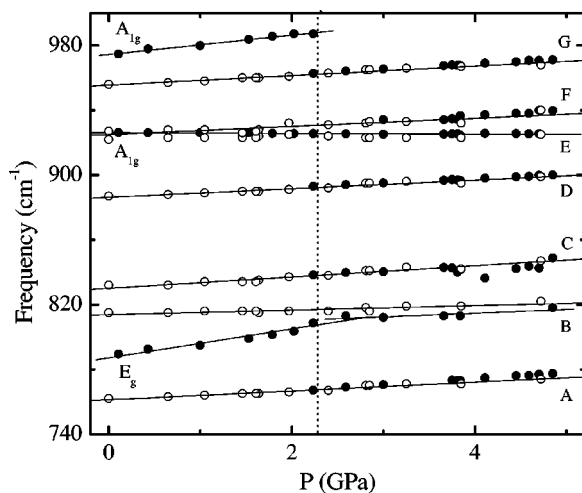

FIG. 4. Frequency vs pressure plot of the most intense bands (in the high frequency region) observed in $KSc(MoO_4)_2$ crystals for compression (solid circles) and decompression (open circles) experiments. The solid lines are linear fits on the data to $\omega(P)=\omega_0+\alpha P$. The vertical dotted line indicates the pressure at about the phase transition takes place.

higher $\partial\omega/\partial P$ values than the modes observed for the high pressure phase, except of the narrow mode at about 926 cm^{-1} that is almost pressure independent (-0.2 $cm^{-1}GPa^{-1}$). Since the frequency of the 926 cm^{-1} mode, as shown by our lattice dynamics calculations, is very sensitive to the Mo–O1 bond length variation, the observed pressure dependence clearly shows that as a result of applied pressure the Mo–O1 bond length does not change. The applied pressure must result, however, in significant shortening of the Mo–O2 bond length, as evidenced through the strong pressure dependence of the 788 and 975 cm^{-1} modes (see Table IV). Our lattice dynamics calculations show that the shortening of the Mo–O2 bond length from 1.8533 to 1.8325 Å results in 40.2, 3.2, 57.0, and 4.1 cm^{-1} upshifts for the 975, 926, 788, and 327 cm^{-1} modes, respectively, whereas the 348 cm^{-1} mode should experience a 14.6 cm^{-1} downshift. As can be seen the performed calculations predict quite well the pressure dependence of the internal modes, showing the strongest dependence for the 788 cm^{-1} mode and weak pressure dependence of the 926 cm^{-1} stretching mode as well as the 327 and 348 cm^{-1} bending modes (see Table IV). Since the number of modes increases when the phase transition takes place, the high pressure phase has a lower symmetry than the starting trigonal phase and this will be further supported by the analysis of translational modes presented in the next paragraph. It is clear from Fig. 4 that for pressures higher than 2.02 GPa a splitting of the stretching modes into 7 components occur. Since there are four stretching vibrations for a MoO_4^{2-} tetrahedron, the observation of 7 components indicates that this new phase has two nonequivalent MoO_4^{2-} units and that the site symmetry of these units is lower (possibly C_1 symmetry) than in the trigonal phase. The lowering symmetry effect also is observed in the low frequency part of the Raman spectra but we will discuss this later on.

Upon releasing pressure the spectrum of the starting trigonal phase was not recovered as can be observed in Fig. 5 and

TABLE IV. Pressure intercepts ω_0 and pressure coefficients α for trigonal and high pressure phase of KSc(MoO$_4$)$_2$ crystals.

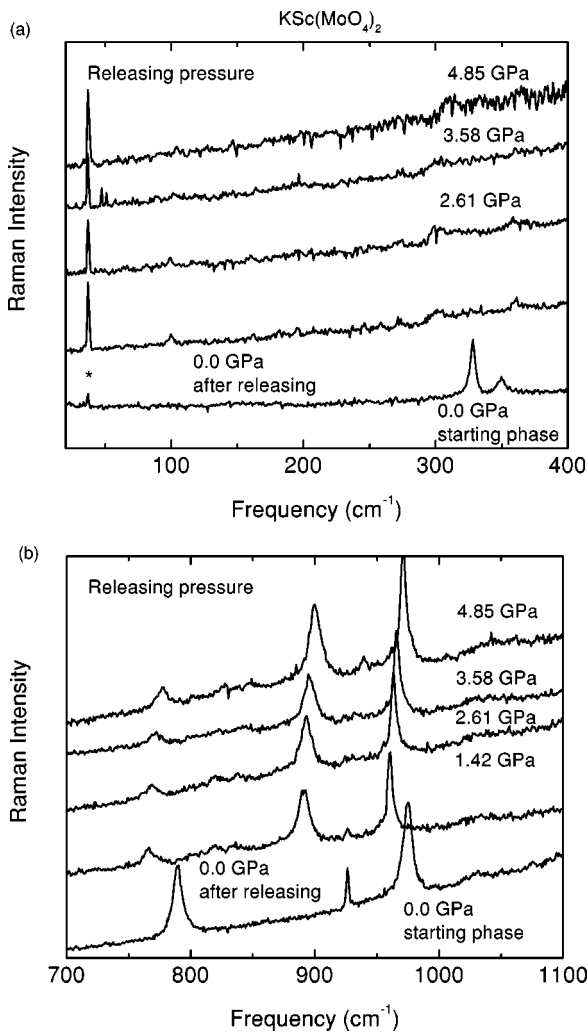| | | | $\omega(P) = \omega_0 + \alpha P$ | | |
| | Trigonal phase | | | High pressure phase | |
Mode	ω_0 (cm^{-1})	α (cm^{-1} GPa^{-1})	Mode	ω_0 (cm^{-1})	α (cm^{-1} GPa^{-1})
E_g	327.4	1.4			
E_g	348.3	2.4			
			A	761	2.7
E_g	788.0	8.9			
			B	813.8	1.4
			C	830.0	3.4
			D	886.3	2.6
A_{1g}	926.1	-0.2	E	926.1	-0.2
			F	925.0	2.5
			G	955.6	2.9
A_{1g}	974.6	3.97			

FIG. 5. Raman spectra of KSc(MoO$_4$)$_2$ crystals recorded at different pressures during decompression experiments. The upper (lower) panel shows the low(high) frequency regions of the spectra. The lower trace in both panels stands for the KSc(MoO$_4$)$_2$ starting phase (before compression). The peak marked with an asterisk in (a) stands for a plasma line from the laser source.

in the ω vs P plots shown in Fig. 4. In order to check the stability of the high-pressure phase, we have monitored the Raman spectra after awaiting for a long time (one week) and the spectra remain exactly the same thus indicating that pressure induced an irreversible phase transition in KSc(MoO$_4$)$_2$. In order to get a fine structure of the Raman spectra for the high pressure phase, we have carried out measurements of the KSc(MoO$_4$)$_2$ sample outside the pressure cell for the sample that has been compressed. By running these experiments we got a signal intense enough for resulting in a well resolved Raman spectra of the high pressure phase. In Fig. 6 we show, for comparison sake, the spectra of the high pressure phase obtained at $P = 4.85$ GPa and at $P = 0$ (outside and inside the pressure cell) after releasing the pressure. It is clear that the three spectra shown in Fig. 6 come from the same phase. The unique difference among them relies on the frequency upshift that is expected since the sample has been probed at different pressure and ω is pressure dependent as shown in Fig. 4. Moreover, we observed a very rich spectra in the lattice mode frequency region [see lower trace in Fig. 6(b)]. By comparing this spectrum with those recorded inside the pressure cell (4.85 GPa and 0.0 GPa after releasing pressure) one can see that they exhibit the same spectral signatures besides the signal to noise ratio is much worse for the spectra recorded for the sample inside the pressure cell.

The spectra recorded outside the pressure cell after compression experiment have much more modes than the spectra recorded at ambient pressure where the KSc(MoO$_4$)$_2$ has a trigonal structure. This large number of modes (33 well resolved peaks) observed at the high pressure compared with the spectra of the trigonal phase (6 well resolved peaks) is due to symmetry lowering effects. According to Table I the translational modes of K and Sc atoms as well as the $A_{2g} \oplus A_{1u}$ librational modes of the MoO$_4^{2-}$ units are Raman inactive in the trigonal phase. Moreover, a number of modes are doubly degenerate in the D_{3d}^3 structure. A phase transition to a lower symmetry, orthorhombic, monoclinic or triclinic, would activate these modes and would lift degeneracy of some vibrational modes thus explaining the large number
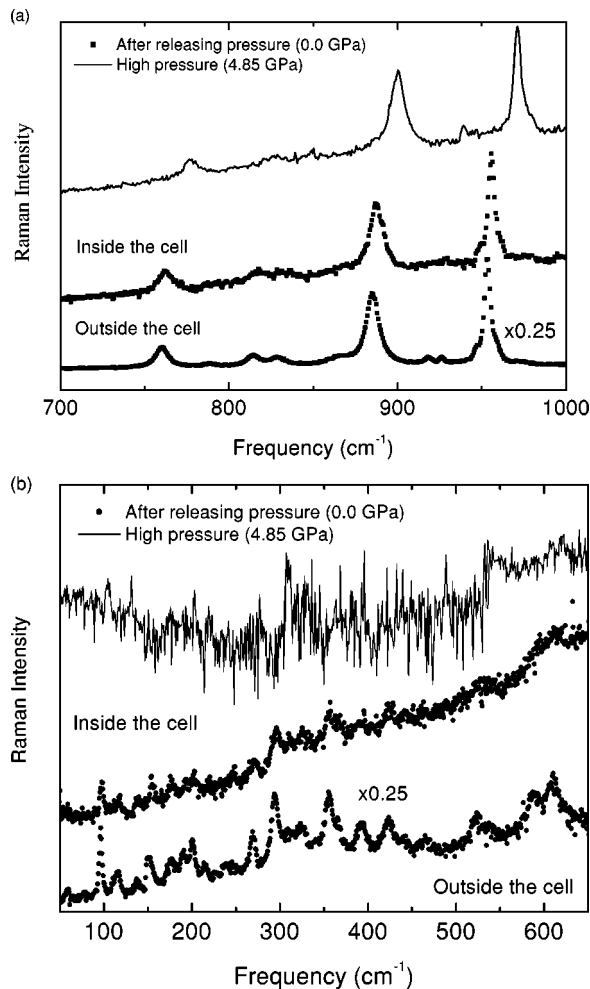
FIG. 6. Raman spectra of $KSc(MoO_4)_2$ crystals recorded at high (solid curves) and ambient pressure (dotted curves) after compression runs showing the irreversibility of the high pressure phase. The upper(lower) panel shows the high(low) frequency regions of the spectra.

of modes observed for the high pressure phase. Previous studies reported on isostructural $KAl(MoO_4)_2$ and $NaAl(MoO_4)_2$ crystals[6] showed that as a result of $D_{3d}^3 \rightarrow C_{2h}^6$ symmetry lowering, the number of internal(lattice) modes increases to 11(8). The same result is observed for the $KSc(MoO_4)_2$ crystal below 260 K.[5,14] It is known that the temperature induced ferroelastic phase transition in trigonal double molybdates and tungstates, including $KSc(MoO_4)_2$, is connected with rotations of the MoO_4^{2-} tetrahedra and shifts of alkali metal atoms from the inversion center (see Otko *et al.*[4]). The trigonal structure becomes unstable with decreasing temperature because the shortening of the interlayer distance leads to an increase in the electrostatic repulsion between oxygen atoms. The same mechanism is most likely responsible also for the observed pressure-induced phase transition since the pressure dependence of stretching modes, discussed in the previous section, clearly indicated significant changes in the Mo–O2 bond length and subsequently the O–O distances with increasing pressure. Indeed, the comparison of the ambient pressure and high pressure

Raman spectra of $KSc(MoO_4)_2$ with the spectra of $KAl(MoO_4)_2$ and $NaAl(MoO_4)_2$ (the replacement of the K cations by smaller Na cations can be regarded as inducing "chemical pressure") shows significant similarities between the behavior of these two groups of compounds. First, the highest frequency stretching mode shifts towards lower frequency by 20–30 cm^{-1}. Second, the sharp line around 930 cm^{-1} seems to be very weakly affected by structural changes. Third, the doubly degenerate modes split. Fourth, the energy gap between stretching and bending modes decreases significantly. Finally, many new bands appear in the lattice modes region.

It is worth noting, however, that although the pressure induced structural changes seem to be connected with rotations of the molybdate tetrahedral MoO_4^{2-} unit, they are much more pronounced than those induced by temperature. In particular, there are two nonequivalent molybdate tetrahedra in the unit cell of the high-pressure phase. Moreover, the observation of much smaller energy gap between bending and stretching modes for the high pressure phase of $KSc(MoO_4)_2$ (~ 150 cm^{-1}) than that found for $NaAl(MoO_4)_2$ (~ 360 cm^{-1}) indicates the presence of significant interactions between the MoO_4^{2-} tetrahedra in the high pressure structure of $KSc(MoO_4)_2$.

It is known that when molybdenium or tungsten atoms are not in a purely tetrahedral coordination, i.e., the tetrahedra are not isolated units but they do interact significantly with each another, the above discussed energy gap decreases. For example, the pressure dependent studies of ZrW_2O_8 showed that as a result of pressure induced phase transition, a significant decrease in the nonbonding $W \cdots O$ distances occurred in this material thereby leading to an increase in bonding strength of these interactions and to develop an energy gap decreasing from 350 cm^{-1} to 200 cm^{-1}.[15,16] Finally, we could argue that although pressure pushes the MoO_4^{2-} units against each other to give rise in interactions between them, the observed bands in the 500–610 cm^{-1} region are not strong, as they usually appear in a wolframite-type structure (octahedral coordination) as found in $LiIn(MoO_4)_2$.[17] In this scenario it is expected to observe some softening in the MoO_4^{2-} stretching modes due to the coupling between the MoO_4^{2-} units. Our results support this assumption because we have observed softening of the modes at about 975 and 788 cm^{-1} when the phase transition occurs [see Figs. 2(b) and 4]. Therefore, we may conclude that the high pressure phase is not a wolframite-type structure, for which very strong interactions between the MoO_4^{2-} ions occur thus promoting a tetrahedral–octahedral Mo coordination change. A definite determination of the high pressure phase symmetry needs x-ray experiments either at high pressures or for the compressed samples and the experiments are under way.

IV. CONCLUSION

In summary, we have presented a high-pressure Raman study of the layered double molybdate $KSc(MoO_4)_2$. A definite assignment of the various Raman active modes have

been achieved by performing lattice dynamics calculations. The very narrow stretching mode, observed at 926 cm^{-1}, involves large stretching motion of the Mo–O1 bond only. This bond projects into the interlayer and interacts weakly with K$^+$ cations only. As a result of these very weak interactions the 926 cm^{-1} mode is practically not sensitive to the applied pressure. In contrast, the pressure strongly affects the Mo–O2 bond lengths and O–O distances. These bond length decreases lead to a further increase in electrostatic repulsion between the oxygen atoms and consequently give rise to the instability of the trigonal structure and any other phase transitions connected with rotations of the molybdate tetrahedra. The pressure dependent Raman studies revealed that the high pressure phase contains two crystallographically nonequivalent MoO$_4^{2-}$ units of low symmetry, possibly C_1. The spectra have revealed some interaction between these molybdate tetrahedra, i.e., as a result of pressure induced phase transition a

significant decrease in the nonbonding Mo$\cdots$O distances is suggested. The presence of these interactions and a higher density of the high pressure phase makes the rotations of the MoO$_4^{2-}$ units more difficult, thus resulting in significantly smaller pressure dependence of the Raman frequencies. This was indeed observed for the high pressure phase in comparison to the low pressure trigonal phase.

*Author to whom correspondence should be addressed. Email address: agsf@fisica.ufc.br

[1] T. Ano, N. Ogata, and Y. Miyaro, J. Catal. **161**, 78 (1996), and references therein.

[2] V. Dmitriev, V. Sinitsyn, R. Dilamian, D. Machon, A. Kuznetsov, E. Ponyatovsky, G. Lucazeau, and H.P. Weber, J. Phys. Chem. Solids **64**, 307 (2003).

[3] D.V.S. Muthu, B. Chen, J.M. Wrobel, A.M.K. Andersen, S. Carlson, and M.B. Kruger, Phys. Rev. B **65**, 064101 (2002).

[4] A.I. Otko, N.M. Nesterenko, and L.V. Povstyanyi, Phys. Status Solidi A **46**, 577 (1976).

[5] N.M. Nesterenko, V.I. Fomin, A.V. Peschanskii, and V.V. Mitkevich, Ferroelectrics **239**, 101 (2000).

[6] M. Maczka, S. Kojima, and J. Hanuza, J. Raman Spectrosc. **30**, 339 (1999).

[7] A. Jayaraman, S.K. Sharma, S.Y. Wong, S.R. Shieh, L.C. Ming, and S.-W. Cheong, J. Raman Spectrosc. **27**, 485 (1996).

[8] M. Maczka, J. Hanuza, S. Kojima, and J.H. Van der Maas, J. Solid State Chem. **158**, 334 (2001).

[9] M.B. Zapart, Phys. Status Solidi A **144**, K23 (1994).

[10] M. Maczka, J. Hanuza, F. Jiang, and S. Kojima, Phys. Rev. B **63**, 144101 (2001).

[11] R.F. Klevtsova and P.V. Kletsov, Kristallografiya **15**, 953 (1970).

[12] M. Maczka, S. Kojima, and J. Hanuza, J. Phys. Soc. Jpn. **68**, 1948 (1999).

[13] R. Nozaki, J.N. Kondo, C. Hirose, K. Domen, A. Wada, and Y. Morioka, J. Phys. Chem. B **105**, 7950 (2001), and references therein.

[14] N.M. Nesterenko, V.I. Fomin, Y.A. Popov, and A. Otko, Sov. J. Low Temp. Phys. **8**, 43 (1982).

[15] J.S.O. Evans, Z. Hu, J.D. Jorgensen, D.N. Argyriou, S. Short, and A.W. Sleight, Science **275**, 61 (1997).

[16] T.R. Ravindran, A.K. Arora, and T.A. Mary, J. Phys.: Condens. Matter **13**, 11 573 (2001).

[17] M. Maczka, J. Hanuza, and A. Pietraszko, J. Solid State Chem. **54**, 498 (2000).